Helicity Observation of Weak and Strong Fields

Mei Zhang

National Astronomical Observatory, Chinese Academy of Sciences, A20 Datun Road, Chaoyang District, Beijing 100012, China (zhangmei@bao.ac.cn)

Abstract. We present in this paper an analysis of a large sample of vector magnetic field measurements. We use data obtained from January 1997 to August 2004 by Huairou Solar Observing Station of the Chinese National Astronomical Observatory. Two physical quantities, α_{best} and current helicity, are calculated and their signs and amplitudes are studied in a search for solar cycle variations. Different from most other studies of this type, we calculate these quantities for weak ($100G<|B_z|<500G$) and strong ($|B_z|>1000G$) fields separately. For weak fields, we find that the signs of both α_{best} and current helicity follow the established hemispheric rule and their magnitudes show a decline with the development of solar cycle. Analysis of strong fields gives an interesting result: Both α_{best} and current helicity present a sign opposite to that of weak fields. Implications of these observations for solar dynamo theory are also briefly discussed in the paper.

Index Terms. Sun; Magnetic field measurement; Magnetic helicity

1. Introduction

Magnetic helicity is a physical quantity that measures the topological complexity of a magnetic field, such as the degree of linkage and/or twistedness in the field (Moffatt 1985, Berger and Field 1984). It has been shown that its total amount is approximately conserved in the Sun even when there is an energy release during fast magnetic reconnection (Berger 1984). This conservation of total magnetic helicity is considered to play an important role in the dynamical processes in the Sun. For example, by considering helicity conservation in the mean-field dynamo process, theories have predicted that solar dynamo would produce opposite helicity signs in the mean field and in the fluctuations (Field et al. 1999, Ossendrijver 2003). It has also been considered that magnetic helicity and its conservation may play an important role in CME dynamics (Low 1999, 2001; Demoulin et al. 2002) where accumulation of total magnetic helicity in the respective northern and southern hemispheres naturally leads to the storage of magnetic energy for CME eruptions (Zhang and Low 2005).

In order to check above theories it is thus important to measure magnetic helicity. However, so far we still cannot directly measure magnetic helicity because so far the photosphere is the only layer that we can measure vector magnetic fields with reasonable temporal and spatial resolutions. On the other hand, by calculating α and current helicity from observed photospheric vector magnetograms we do get a glimpse of the properties of magnetic helicity in the Sun. For example, from photospheric vector magnetic field observations we learn that magnetic fields emerging from the solar convection zone to the photosphere are already significantly twisted (Kurokawa 1987, Leka et al. 1996) and statistically these fields possess a positive helicity sign in the southern hemisphere and a negative helicity sign in the northern hemisphere (Rust 1994, Pevtsov et al. 1995, Bao and Zhang 1998). These observations in return give us implications on how the magnetic helicity is produced in the convection zone (Berger and Ruzmaikin 2000) and how the helicity conservation may play a role in balancing the twist and writhe helicity in an originally untwisted flux rope (Longcope et al. 1998).

In this paper, we intend to check the observational evidence of another property derived from helicity conservation, that is, the solar dynamo produces opposite helicity signs in the mean field and in the fluctuations (Field et al. 1999). We also use the photospheric vector magnetic field measurements to derive our studied physical quantities. But different from other works, we separate our studied fields into two parts: strong magnetic fields and weak magnetic fields. We organize our paper as follows. In Section 2, we describe our observation and data reduction. In Section 3, we present our analysis and discussions. We conclude our paper with a brief summary in Section 4.

2. Observation and data reduction

The tunable birefringent filter of the solar telescope magnetograph at the Huairou Solar Observing Station of the National Astronomical Observatory can be aimed at different passbands for different observations (Ai and Hu, 1986). For the photospheric observations we used in this paper, the passband of the filter is set in the FeIλ5324 line: at 0.075Å from the line center for the measurement of longitudinal

magnetic field (Stokes V) and at the line center for the measurement of transverse magnetic fields (Stokes Q and U). The equivalent width of FeIλ5324 line is 0.344Å and the FWHM of the filter passband is 0.15 Å. More information of the magnetograph and calibration can be found in Ai et al. (1982), Zhang and Ai (1986) and Su and Zhang (2004).

A dataset of the photospheric vector magnetograms obtained by above magnetograph during the period of 1997 January 1 to 2004 August 31 is analyzed in this paper. This dataset contains 17200 vector magnetograms and covers almost all active regions appeared during this period. We calibrated each vector magnetogram according to Ai et al. (1982) and solve the 180-degree ambiguity by setting the directions of transverse fields most closely to a current-free field.

We calculated two physical quantities, α_{best} and current helicity, of each magnetogram, as helicity indicators. Following Pevtsov et al. (1995) we calculated α_{best} as a best-fit single value where $\nabla\times\mathbf{B}=\alpha_{best}\mathbf{B}$. The current helicity ($h_c$) in this paper is defined as $h_c=B_z(\nabla\times\mathbf{B})_z$, which is actually the longitudinal (z) component of the current helicity density at the photosphere (z=0). When calculating these physical quantities we have used only those magnetograms observed within 40 degrees from the disk center and we have also only used those data points whose longitudinal field strengths ($|B_z|$) are greater than 100G and whose transverse field strengths ($|B_x|$ and ($|B_y|$) are both greater than 200G after correcting for projection effects. Note our treatments in data reduction so far are as typical as most other authors in reducing vector magnetograms (Pevtsov et al. 1995, Bao and Zhang 1998, Pevtsov et al. 2001).

Our unique treatment of the data is that we divide our measured magnetic fields into two parts: strong fields whose longitudinal flux densities ($|B_z|$) are greater than 1000G and weak fields whose longitudinal flux densities ($|B_z|$) are between 100G and 500G. Our strong fields are then mainly consisted of the central part of sunspots and our weak fields are mainly of enhanced magnetic networks. We calculated the α_{best} and current helicity for strong and weak fields separately. This treatment has led us to interesting results that we describe in the following.

3. Analysis and discussions

3.1 Comparison with previous studies

Before we proceed to present our results it is useful to check our data reduction of this dataset with previous studies. We selected a sub-sample from our dataset, containing observations made between 1997 July to 2000 September, in order to compare with Pevtsov et al. (2001) where α_{best} and current helicity were also calculated for the same period of time. The difference is that their data were obtained by the Haleakala Stokes Polarimeter (HSP) at Mees Solar Observatory.

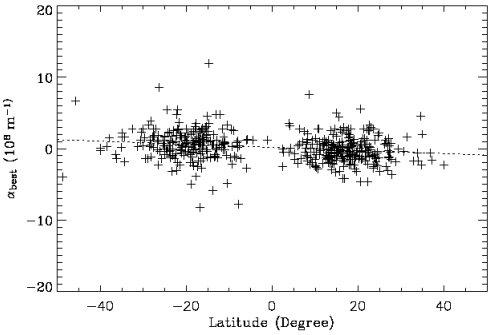

Fig. 1. Latitudinal profile of α_{best} for 391active regions observed by Huairou magnetograph between 1997 July and 2000 September.

Figure 1 presents the latitudinal profile of α_{best} for the 391 active regions observed by Huairou magnetograph between 1997 July and 2000 September. Each point presents an average of α_{best} when multiple magnetograms of the same active region were obtained. The dashed line shows the least-square best-fit linear function of these α_{best} values. Note in producing this figure we did not separate the weak and strong fields but instead used all data points with $|B_z|>100$G and $|B_x, B_y|>200$G in order to make a reasonable comparison with Pevtsov et al. (2001). Our Figure 1 presents a similar tendency of α_{best} variations with latitudes as that in Figure 1 of Pevtsov et al. (2001). This shows a good consistence between the two datasets.

Out of our 391 active regions during this period, 58.9% of 214 active regions in the northern hemisphere have $\alpha_{best}<0$ and 67.2% of 117 active regions in the southern hemisphere have $\alpha_{best}>0$. These numbers are consistent with the numbers of 62.9% and 69.9% for northern and southern hemispheres respectively in Pevtsov et al. (2001).

Our data shows no hemispheric tendency by current helicity. 44.4% of 214 active regions in the northern hemisphere have $h_c<0$ and 45.8% of 117 active regions in the southern hemisphere have $h_c>0$. Note in Pevtsov et al. (2001) a much weaker tendency is also found with numbers of 50% and 57.5% for their h_c values in the northern and southern hemispheres respectively. They contribute this difference to the Faraday rotation. But we suggest the difference is largely (although possibly not all) because of a physical point on which we will return to address below.

3.2 Helicity observation of weak fields

Figure 2 presents our result of solar cycle variations of α_{best} (top panel) and current helicity (middle panel) for weak fields ($100G<|B_z|<500G$). Each point in these plots is a weighted average of α_{best} or current helicity for active regions observed during one year. For active regions in the southern hemisphere the weight is set to *1* and for active regions in the

northern hemisphere the weight is set to *-1*. The weighted averages then indicate the magnitudes of α_{best} or current helicity averaged over the global surface during a whole year, assuming the northern and southern hemispheres have opposite helicity signs. We see that the averages of both α_{best} and current helicity have positive signs except for the Year 2004. This tells us that both α_{best} and current helicity for weak fields obey the established hemispheric rule during most years of the solar cycle. The averages of α_{best} and current helicity for Year 2004 are negative, which indicates that the usual hemispheric rule is violated in this year. This is consistent with Hagino and Sakurai (2005) where they also found the usual hemispheric rule is not obeyed during solar minimums.

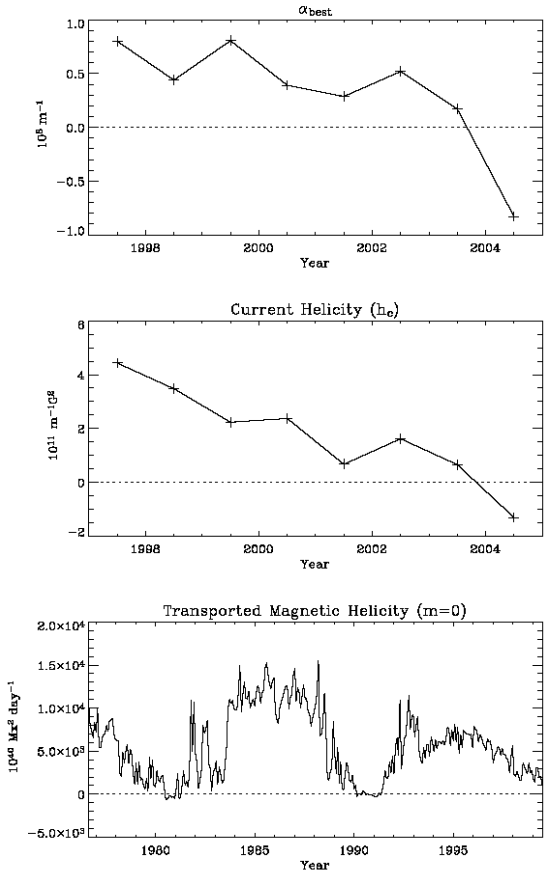

Fig. 2. Solar cycle variations of weighted averages of α_{best} (top panel) and current helicity (middle panel) for weak fields ($100G<|B_z|<500G$). Bottom panel: Calculated helicity transfer of the m=0 mode, created by differential rotation in the interior, into the southern hemisphere. Adopted from Berger and Ruzmaikin (2000).

Figure 2 also presents a rough tendency of a decrease of the magnitudes of α_{best} or current helicity with the development of solar cycle. We notice in Berger and Ruzmaikin (2000), helicity production in solar interior by differential rotation is calculated and their calculation also shows a similar decrease of magnitudes of the helicity transported into the northern or southern hemisphere. This is shown in the bottom panel of Figure 2 where the helicity transported into the southern hemisphere by the m=0 mode is re-plotted, with data taken from Berger and Ruzmaikin (2000). This interesting consistence seems to suggest that differential rotation is the source of helicity production in solar interior although we are not sure because we do not know whether the α effect will also produce the same tendency.

Another interesting implication from Figure 2 is that, whereas we usually consider helicity variations as a function of latitudes as we do in Figure 1, we are actually not sure whether the helicity variation is rather associated with solar cycle dependence than associated with latitude dependence.

3.3 Helicity observation of strong fields

For strong magnetic fields ($|B_z|>1000G$) calculation of weighted averages of α_{best} and current helicity presents an interesting result as shown in Figure 3. All weighted averages of α_{best} and most of the current helicity are negative, which means they do not follow the usual hemispheric rule. This also shows that strong fields have a helicity sign opposite to that of weak fields.

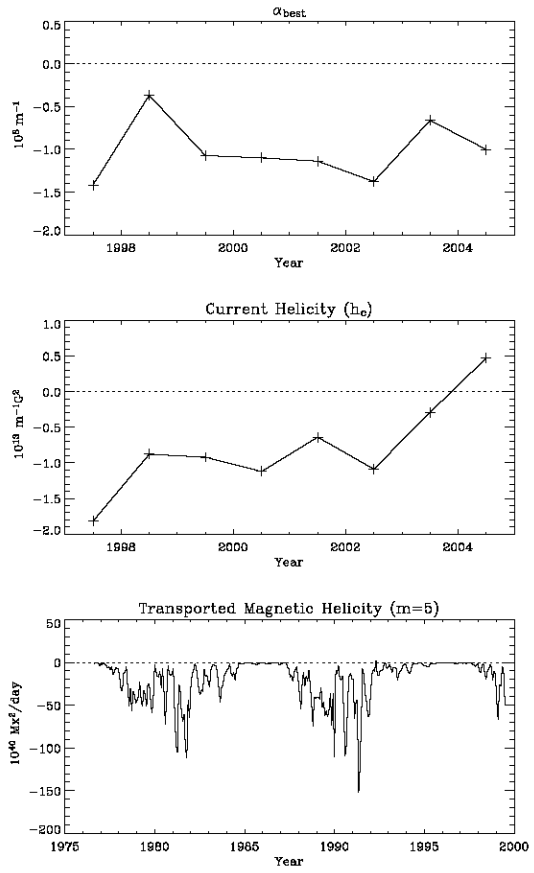

Fig. 3. Top and middle panels: Same as in Figure 2 but for strong fields ($|B_z|>1000G$). Bottom panel: Same as in Figure 2 but for m=5 mode.

If we interpret our weak and strong fields represent large and small scales respectively, then our observation seems to support the theory that solar dynamo would produce opposite helicity signs in the mean field and in the fluctuations. It is also interesting to notice that in Berger and Ruzmaikin (2000)

the higher modes helicity, such as the m=5 mode re-plotted in Figure 3, also has a sign opposite to that of the m=0 mode. So, if we interpret their low-degree (such as m=0) and high-degree (such as m=5) modes correspond to our weak and strong fields respectively their calculation again shows a consistence with our observation.

The observation that strong fields have a helicity sign opposite to that of weak fields may also help us understand why α_{best} usually shows a better hemispheric rule than current helicity if both quantities are calculated from vector magnetograms of the whole field. It is because when we calculate α_{best} all data points are given the equal weight so the resultant α_{best} presents the sign of weak fields, which dominate over strong fields by numbers. But when we calculate the current helicity as $h_c=B_z(\nabla\times\mathbf{B})_z=\alpha B_z^2$ we have attributed a weight of B_z^2 to each point so that the current helicity of weak and strong fields almost cancels each other. This is because strong fields are less dominant by numbers but stronger by field strengths whereas weak fields are weaker by field strengths but are more dominant by numbers.

It has been suggested that Faraday rotation contributes to the difference between α_{best} and current helicity. We suggest the main reason is the opposite helicity signs between weak and strong fields. Su and Zhang (2006, in preparation) recently did a calculation and it shows that whereas Faraday rotation may rotate the transverse fields to 20 - 30 degrees, the resultant α values are less influenced, with changes of α values all less than a few percentages. Another comment is that if Faraday rotation is the reason of the difference we should not see the difference in the dataset obtained by spectrograph-type magnetographs where the effect of Faraday rotation can be taken care of by inversion methods. But the difference is observed in Pevtsov et al. (2001) where HSP data are used. We have recently checked several active regions observed by ASP/HAO. Similar feature of opposite helicity signs between weak and strong fields is also found, although not in every region examined. A further confirmation is needed based on a large sample from another magnetograph such as ASP.

4. Summary

A sample of 17200 photospheric vector magnetograms of active regions observed from January 1997 to August 2004 is analyzed in this paper. Different from other works, we calculate the helicity indicators, α_{best} and current helicity, for weak ($100G<|B_z|<500G$) and strong ($|B_z|>1000G$) fields separately.

By analyzing this dataset we find that: 1) For weak magnetic fields, the signs of both α_{best} and current helicity follow the established hemispheric rule except during Year 2004. The magnitudes of their weighted averages show a tendency of decreasing with the development of solar cycle. 2) For strong magnetic fields, both α_{best} and current helicity show a helicity sign opposite to that of weak fields.

Upon the interpretation that weak and strong fields represent small and large scales respectively, our observation seems to be consistent with the calculation made by Berger and Ruzmaikin of the helicity production by differential rotation. Our results also seem to support the theory that solar dynamo would produce opposite helicity signs in the mean field and in the fluctuations.

.

Acknowledgments. I thank Mitchell Berger for providing his calculation results that was used in Figures 2 and 3 of this paper. My special thanks to my colleagues in Huairou Solar Observing Station for their years-long endeavors in acquiring vector magnetograms that makes this work possible. This work was supported by the One-Hundred-Talent Program of the Chinese Academy of Sciences, the Chinese National Science Foundation under Grant 10373016, and the U.S. National Science Foundation under Grants SHINE ATM-0203489 and ATM-0548060.

References

G. X. Ai, W. Li and H. Q. Zhang, 1982, Chinese Astronomy and Astrophysics, 6, 129
G. X. Ai and Y. Hu, 1986, Acta Astron. Sin, 27, 173
S. D. Bao and H. Q. Zhang, 1998, ApJ, 496, L43
M. A. Berger, 1984, Geophys. Astrophys. Fluid Dynamics, 30, 79
M. A. Berger and G. B. Field, 1984, J. Fluid Mech., 147, 133
M. A. Berger and A. Ruzmaikin, 2000, J. Geophys. Res., 105, 10481
P. Demoulin, C. H. Mandrini, L. van Driel-Gesztelyi, et al.: 2002, A&A, 382, 650
G. B. Field, E. G. Blackman and H. Chou, 1999, ApJ, 513, 638
M. Hagino and T. Sakurai, 2005, PASP, 57, 481
H. Kurokawa, 1987, Sol. Phys., 113, 259
K. D. Leka, R. C. Canfield, A. N. McClymont and L. van Driel-Gesztelyi, 1996. ApJ, 462, 547
D. W. Longcope, G. H. Fisher and A. A. Pevtsov, 1998, ApJ, 507, 417
B. C. Low, 1999, in *Magnetic Helicity in Space and Laboratory Plasmas*, ed. by M. R. Brown, R. Canfield & A. Pevtsov (Washington D.C. : AGU), 25
B. C. Low, 2001, J. Geophys. Res., 106, 25141
H. K. Moffatt, 1985, J. Fluid Mech., 159, 359
M. Ossendrijver, 2003, Astron. Astrophys. Rev., 11, 287
A. A. Pevtsov, R. C. Canfield and S. M. Latushko, 2001, ApJ, 549, L261
A. A. Pevtsov, R. C. Canfield and T. R. Metcalf, 1995, ApJ, 440, L109
D. M. Rust, 1994, Geophys. Res. Lett., 21, 241
J. T. Su and H. Q. Zhang, 2004, Chin. J. Astron. Astrophys., 4, 365
H. Q. Zhang and G. X. Ai, 1986, Acta Astron. Sin., 27, 217
M. Zhang and B. C. Low, 2005, ARAA, 43, 103